Lucío, MI.; Pichler, F.; Ramírez, JR.; De La Hoz, A.; Sánchez-Migallón, A.; Hadad, C.; Quintana, M.... (2016). Triazine-Carbon Nanotubes: New Platforms for the Design of Flavin Receptors. Chemistry - A European Journal. 22(26):8879-8888. https://doi.org/10.1002/chem.201600630

Triazine-Carbon Nanotubes: New Platforms for the Design of Flavin Receptors

María Isabel Lucío,[a, b] Federica Pichler,[a, b] José Ramßn Ramírez,[a] Antonio de la Hoz,[a] Ana Sánchez-Migallßn,[a] Caroline Hadad,[b] Mildred Quintana,[c] Angela Giulani,[b] Maria Victoria Bracamonte,[b, d] Jose L. G. Fierro,[e] Claudio Tavagnacco,[b] María Antonia Herrero,[a] Maurizio Prato,[b] and Ester Vázquez*[a]

Abstract: The synthesis of functionalised carbon nanotubes as receptors for riboflavin (RBF) is reported. Carbon nanotubes, both single-walled and multi-walled, have been functionalised with 1,3,5-triazines and *p*-tolyl chains by aryl radical addition under microwave irradiation and the derivatives have been fully characterised by using a range of techniques. The interactions between riboflavin and the hybrids were analysed by using fluorescence and UV/Vis spectroscopic techniques. The results show that the attached functional groups minimise the *p*-*p* stacking interactions between riboflavin and the nanotube walls. Comparison of *p*-tolyl groups with the triazine groups shows that the latter have stronger interactions with riboflavin because of the presence of hydrogen bonds. Moreover, the triazine derivatives follow the Stern–Volmer relationship and show a high association constant with riboflavin. In this way, artificial receptors in catalytic processes could be designed through specific control of the interaction between functionalised carbon nanotubes and riboflavin.

Introduction

Flavoproteins are redox enzymes related to metabolic processes, electron transfer and regulation of neurotransmitters.[1] The interdependence between redox events and molecular recognition is a prevalent theme when studying these systems. The flavin cofactor of proteins is the active site in the catalytic processes and its redox behaviour depends on the covalent and noncovalent interactions with the apoenzyme. Therefore, modulation of the environment of flavins can be used to set their selectivity towards a specific analyte[2] and to understand the behaviour of enzymes. Historically, the most widely studied flavin has been riboflavin (RBF) because of its chemical and biological versatility.[3] Covalent attachment of flavins to enzymes is known to enhance selectively a reaction pathway and suppress unwanted side reactions.[4] As a consequence, different covalent modifications have been carried out on the central nucleus of flavins to study their versatility in the design of sensors and alterations in the redox[5] and fluorescence[6] responses have been observed. Similarly, several receptors have been developed to observe the molecular recognition of flavins by noncovalent approaches.[7] For example, the 2,4-diamine-1,3,5-triazines are useful because they have an appropriate D (H-donor)-A (acceptor) matrix to form hydrogen bonds with flavins.[8] The 1,3,5-triazine nucleus is attractive in supramolecular chemistry because of the possibility of forming multiple noncovalent interactions[9] by coordinate bonds,[10] electrostatic interactions,[11] hydrogen bonds,[12] and *p*-*p* stacking.[13,14] In addition, from a synthetic point of view, these systems can be easily modified.[15–18]

It is known that three-dimensional (3D) patterns, such as silicate matrices, effectively replicate both the isolation and preorganisation found in the active sites of flavoenzymes.[19] Accordingly, the fabrication of 3D structures could make a difference in the recognition processes of flavins and, apart from the biological mimics, the flavin-receptor complex could also be used in the design of sensors and new catalysts.[20]

[a] *Dr. M. I. Lucío, F. Pichler, Dr. J. R. Ramírez, Prof. A. de la Hoz, Dr. A. Sánchez-Migallón, Dr. M. A. Herrero, Dr. E. Vázquez*
Departamento de Química Orgánica, Inorgánica y Bioquímica, Facultad de Ciencias y Tecnologías Químicas
IRICA Universidad de Castilla-La Mancha Campus Universitario, 130/1 Ciudad Real (Spain)
E-mail: Ester.Vazquez@uclm.es

[b] *Dr. M. I. Lucío, F. Pichler, Dr. C. Hadad, A. Giulani, Dr. M. V. Bracamonte, Prof. C. Tavagnacco, Prof. M. Prato*
Dipartimento di Scienze Chimiche e Farmaceutiche Center of Excellence for Nanostructured Materials (CENMAT) & Italian Interuniversity Consortium on Materials Science and Technology (INSTM - Unit of Trieste) Università degli Studi di Trieste Piazzale Europa 1, 3412/ Trieste (Italy)

[c] *Dr. M. Quintana*
Instituto de Física Universidad Autßnoma de San Luis Potosí Manuel Nava 6, Zona Universitaria /8290, San Luis Potosí, SLP (Mexico)

[d] *Dr. M. V. Bracamonte*
Instituto de Física Enrique Gaviola (CONICET) and FaMAF
Universidad Nacional de Cßrdoba Medina Allende s/n, X5000HUA Cßrdoba (Argentina)

[e] *Prof. J. L. G. Fierro*
Instituto de Catálisis y Petroleoquímica CSIC Cantoblanco
28049 Madrid (Spain)

Carbon nanotubes (CNTs) have been applied in different fields such as electronics,[21] biomedicine[22] and sensor building.[23] The characteristic that makes these materials special is the combination of dimension, structure, and topology, which translates into a whole range of superior properties.[24] Moreover, these materials have a large surface area that can be easily modified in different ways.[25] Covalent functionalisation is a helpful tool to immobilise different useful molecules to build supramolecular structures.[26] In addition, the electrochemical reactivity of some molecules—as well as some electron-transfer processes—are known to be improved by carbon nanotubes, thus making them attractive for the design of biosensors.[27]

We report here the synthesis and noncovalent interactions of triazine-carbon nanotube derivatives with RBF. Both single-walled carbon nanotubes (SWCNTs) and multi-walled carbon nanotubes (MWCNTs) were functionalised by a radical arylation with microwave activation. Different functional groups were immobilised, namely 1,3,5-triazine chains, which are capable of forming hydrogen bonds, and *p*-tolyl chains, which cannot participate in this type of interaction. The characterisation of all of the derivatives was carried out by using a range of techniques such as thermogravimetric analysis (TGA), Raman spectroscopy, UV/Vis/NIR spectroscopy, transmission electron microscopy (TEM) and X-ray photoelectron spectroscopy (XPS). As a further step in understanding the molecular recognition processes, the triazine-functionalised MWCNTs were applied as synthetic hydrogen-bond receptors and their interactions with RBF were analysed.

Results and Discussion

Synthesis and Characterisation of Carbon Nanotube Derivatives

There are a very few examples in which triazine moieties are attached to nanotubes, and most of these concern noncovalent modifications.[28–30] Two kinds of nanotube derivatives were prepared (Scheme 1) with the aim of comparing the behaviour of covalent triazine-functionalised carbon nanotubes with nanotubes functionalised to the same extent but without the possibility of forming hydrogen bonds.

Triazine 1 or *p*-toluidine (2) were reacted with pristine HiPco® SWCNTs under the conditions described in the experimental section to give SWCNTs-1 and SWCNTs-2. Thermogravimetric analysis shows the weight loss from samples as the temperature increases. The TGA results for SWCNTs-1 and SWCNTs-2 are shown in Figure 1a. The weight loss at 600 °C can be used to quantify the number of functional groups attached to the carbon nanotube. SWCNTs-1 showed a weight loss of 14.5 % and this corresponds to 392 *m*mol of functional groups per gram of carbon nanotube. The degree of functionalisation is 1 functional group per 181 carbon atoms. SWCNTs-2 showed a weight loss of 15.7 %, which corresponds to 934 *m*mol of functional groups per gram of carbon nanotube. This corresponds to 1 functional group per 75 carbon atoms. The higher degree of functionalisation can be attributed to the small size of the *p*-tolyl chain when compared with the sterically more hindered triazine unit.[31,32] The electron-withdrawing properties of the triazine ring and the lower solubility of triazine 1 may also reduce its reactivity.[33,34]

Raman spectroscopy provides information about the covalent functionalisation of carbon nanotubes. The increase in the D-band at 1314 cm^{-1} can be related to the introduction of sp^3 defects into the sp^2 network of the nanotube.[35] The Raman spectra of pristine and functionalised SWCNT derivatives are shown in Figure 1 b. SWCNTs-1 exhibits a more intense D-band than p-SWCNTs and a more intense band is observed for SWCNTs-2 as the degree of functionalisation increases. These results are consistent with those of the TGA analysis.

Both SWCNT derivatives were analysed by UV/Vis spectroscopy, which is an excellent method to monitor the electronic perturbation of nanotubes. The van Hove singularities of pristine nanotubes disappeared due to rehybridisation of the sp^2

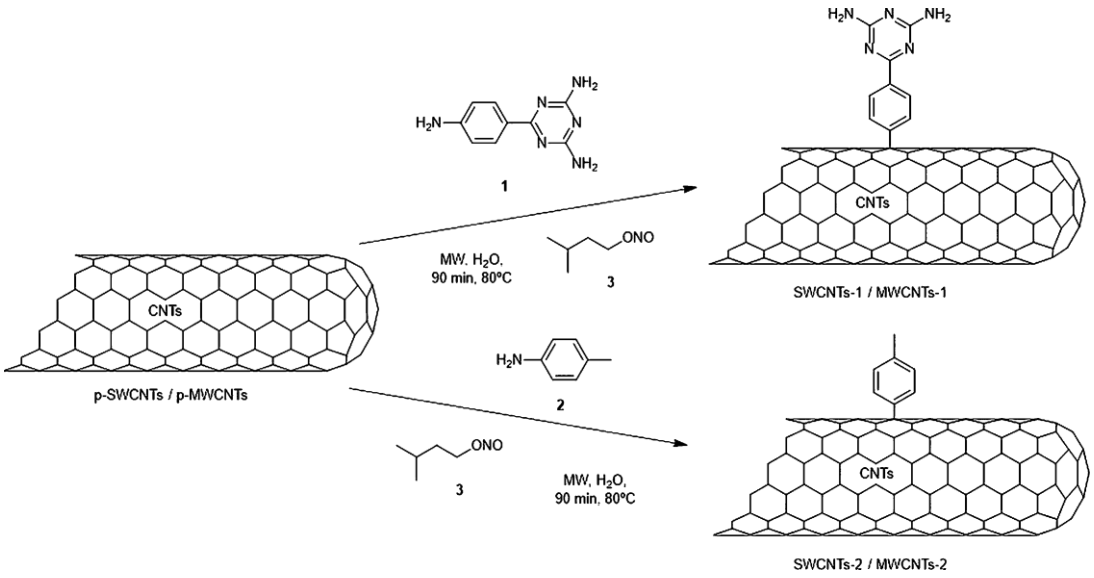

Scheme 1. Functionalisation of p-SWCNTs and p-MWCNTs.

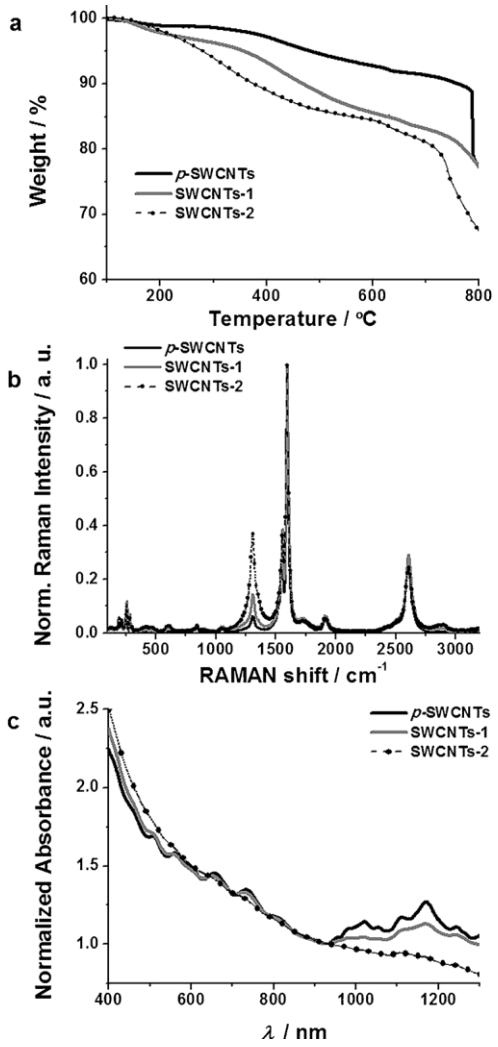

Figure 1. a) Thermogravimetric analysis of p-SWCNTs, SWCNTs-1 and SWCNTs-2. b) Normalised Raman spectra of p-SWCNTs, SWCNTs-1 and SWCNTs-2 by using a laser source at 633 nm. (c) UV/Vis/NIR absorption spectra of p-SWCNTs, SWCNTs-1 and SWCNTs-2 in solutions of sodium dodecyl sulfate (2%) normalised to the local minimum at 930 nm.

carbon atoms to sp^3 in the functionalised carbon nanotubes.[31] A decrease in the intensity of the van Hove bands from p-SWCNTs to SWCNTs-1 and SWCNTs-2 can be observed in Figure 1c because of the increase in the extent of functionalisation. This effect is more evident in SWCNTs-2 because of the higher degree of functionalisation in comparison to SWCNTs-1. The different derivatives were also analysed by X-ray photoelectron spectroscopy (XPS). This semiquantitative technique provides information about the elemental composition of the sample as well as the types of bonds present.[36] As expected, the SWCNTs-2 derivative did not contain nitrogen and the hybrid SWCNTs-1 contained 2.7% nitrogen, thus confirming the functionalisation (Table S1). The N1s peak was deconvoluted into two contributions at 398.3 and 400.1 eV (Figure S1). These were assigned to the photoelectrons emitted by the N=C and N—C bonds present in the triazine rings, respectively. Furthermore, the percentage of nitrogen (2.7%) corresponds to 386 *m*mol of functional groups per gram of carbon nanotube, which is a value that is consistent with that obtained by TGA analysis (392 *m*mol of functional groups per gram of carbon nanotube).

Once the reaction had been successfully carried out with SWCNTs and the products were fully characterised, p-MWCNTs were functionalised with the same organic chains to yield derivatives MWCNTs-1 and MWCNTs-2. The TGA traces for MWCNT derivatives versus p-MWCNTs are shown in Figure S2. MWCNTs-1 exhibited a weight loss of 13 % and this corresponds to 667 *m*mol of functional group per gram of carbon nanotube. The degree of functionalisation is 1 functional group per 110 carbon atoms. MWCNTs-2 showed a weight loss of 11% at 600 8C, which corresponds to 1178 *m*mol of functional group per gram of carbon nanotube. This equates to 1 functional group per 61 carbon atoms. The reaction with *p*-toluidine 2 introduces more functional groups than the reaction with triazine 1, as observed with SWCNTs. Functionalised MWCNTs were also analysed by XPS. As expected, MWCNTs-2 did not contain nitrogen and MWCNTs-1 contained 5.0 % nitrogen, which corresponds to 714 *m*mol of functional groups per gram of carbon nanotube. This value is consistent with that obtained by TGA analysis (667 *m*mol of functional groups per gram of carbon nanotube) (Table S1).

The higher solubility of the final MWCNT derivatives in water in comparison with the SWCNT derivatives, led us to use the former nanotubes to analyse the molecular recognition of RBF.

It is known that the degree of functionalisation is an important factor when the behaviour of CNTs is studied. With the aim of comparing the influence of the types of functional groups, three successive addition reactions were carried out with triazine 1 on the same MWCNT sample. Similar degrees of functionalisation were obtained in the hybrid with triazine and the hybrid with *p*-tolyl groups. The TGA data for the latter derivative, which is denoted as MWCNTs-3, are shown in Figure S2 along with those of the other MWCNT derivatives. The degree of functionalisation of each MWCNT derivative is summarised in Table 1.

It is known that functionalised carbon nanotubes that can form hydrogen bonds in AD-DA (acceptor donor-donor acceptor) systems produce good dispersions in aprotic polar systems such as *N*,*N*-dimethylformamide (DMF), whereas they self-assemble to form superstructures in solvents in which they do not form hydrogen bonds, such as dichloromethane.[37] Consequently, the different dispersibility of the nanotubes in different solvents provides an insight into the kind of interactions between them and the type of functional groups. Hence, the behaviour of MWCNTs-1, MWCNTs-2 and MWCNTs-3 in different solvents was analysed by transmission electron microscopy (Figure 2). Both triazine-MWCNT derivatives formed good dispersions in water, MWCNTs-1 (Figure 2 a) and MWCNTs-3 (Figure 2 b), because of hydrogen-bonding interactions between the organic chains and the solvent. However, the *p*-tolyl-functionalised nanotubes MWCNTs-2 formed aggregates in water (Figure 2 c) as interactions with the solvent did not occur, whereas in nonpolar solvents such as 1,1,2,2-tetrachloroethane the opposite behaviour was observed. The triazine-functional-

Table 1. Summary of the functionalised MWCNTs.

Product	Structure	Weight loss [%][a]	FGC[b]	[*m*mol/g][c]
MWCNTs-1	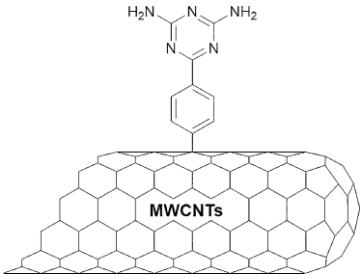	13	110	667
MWCNTs-2	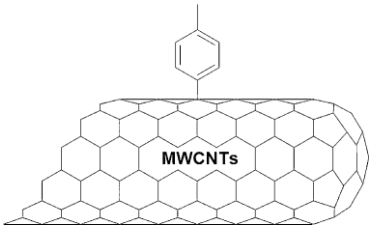	11	61	1178
MWCNTs-3	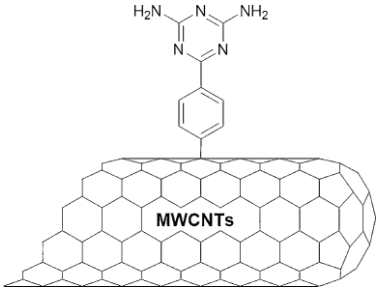	19.5	63	1056

[a] TGA weight loss (%) at 600 °C. [b] Functional group coverage : Number of carbon atoms per functional group = $[(100 - \%_{weightloss}) \cdot M_{functionalgroup}]/12\ \%_{weightloss}$. [c] *m*mol of functional group per gram of carbon nanotube.

ised nanotubes, MWCNTs-1 and MWCNTs-3, self-assembled because of hydrogen-bonding interactions between the functional groups (Figure 2 d, e), whereas the *p*-tolyl-functionalised nanotubes MWCNTs-2 formed a very good dispersion (Figure 2 f).

Molecular Recognition

The study of the molecular recognition of flavins by a receptor is important in the development of sensors as well as in the development of chemical models to understand the role of the noncovalent interactions in enzymatic processes. To obtain a qualitative idea of the interaction between triazine-functionalised carbon nanotubes MWCNTs-1 and RBF, an excess of RBF (5 mg) was added to a 1,1,2,2-tetrachloroethane solution of MWCNTs-1 (20 mL, $2.5 \cdot 10^{-2}$ mg mL^{-1}) and, after washing the mixture, the recognition processes were analysed by TEM. High dispersibility of nanotubes after the addition of RBF can be observed in Figure 3. As expected, the triple ADA-DAD hydrogen-bonding interactions between the functional groups of the nanotubes and RBF break the bundles.

In general, the methodologies used to observe the molecular recognition are based on physical and chemical changes in the receptor system when it interacts with the acceptor system. Numerous studies have been carried out to analyse the recognition of flavin by different receptors and, for example, the quenching of its fluorescence,[38,39] the shift of bands in the UV spectra,[40] the shift of peaks in the IR spectra[41] and NMR spectra[8] or the modification of the redox potential by cyclic voltammetry[42] have been observed. In particular, the linear optical properties of RBF have been widely studied.[43–45]

The UV/Vis spectra from a titration of RBF with increasing concentrations of MWCNTs-3 in water are shown in Figure 4.

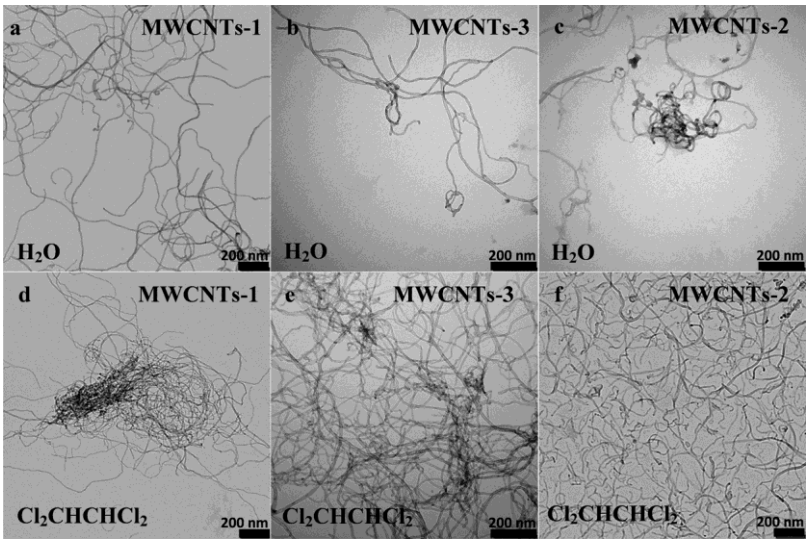

Figure 2. TEM Images of a) MWCNTs-1 in H_2O, b) MWCNTs-3 in H_2O, c) MWCNTs-2 in H_2O, d) MWCNTs-1 in 1,1,2,2-tetrachloroethane, e) MWCNTs-3 in 1,1,2,2-tetrachloroethane, and f) MWCNTs-2 in 1,1,2,2-tetrachloroethane. The concentration of nanotubes in all samples was $2.5 \cdot 10^{-2}$ mgmL^{-1}.

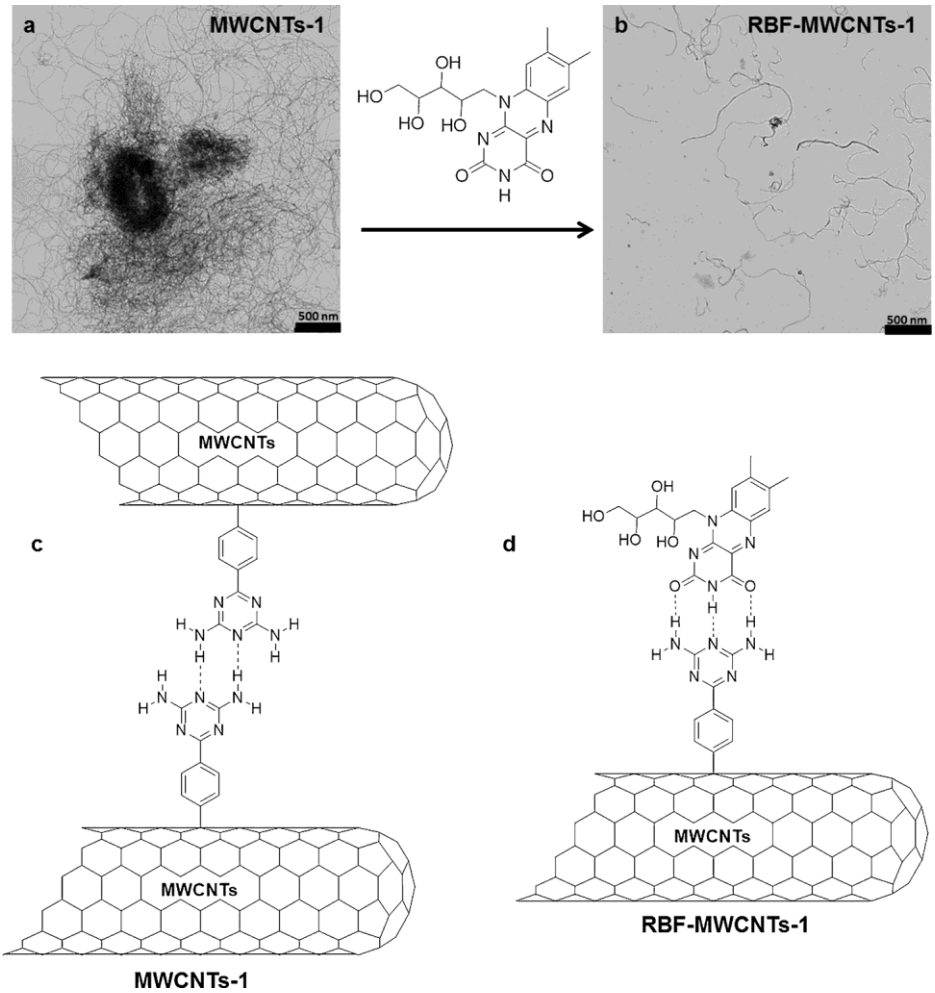

Figure 3. TEM Images of an MWCNTs-1 solution in 1,1,2,2-tetrachloroethane ($2.5 \cdot 10^{-2}$ mgmL^{-1}) a) before and b) after the addition of an excess of RBF. Expected interaction between MWCNTs-1 c) before and d) after the addition of RBF in 1,1,2,2-tetrachloroethane.

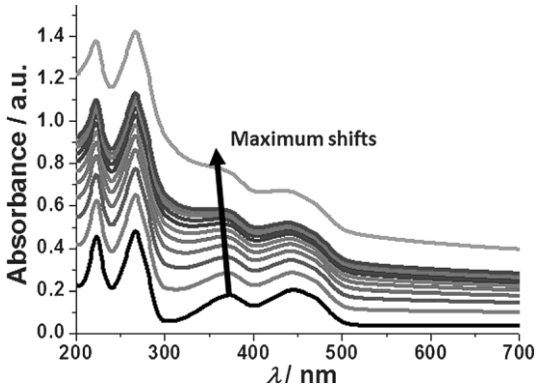

Figure 4. UV/Vis spectra showing a monotonic increase in intensity of RBF with increasing concentration of MWCNTs-3. [RBF] = $5.0 \cdot 10^{-3}$ mg mL^{-1}, [MWCNTs-3] = 0, $1.7 \cdot 10^{-3}$, $2.9 \cdot 10^{-3}$, $3.7 \cdot 10^{-3}$, $4.4 \cdot 10^{-3}$, $5.0 \cdot 10^{-3}$, $5.5 \cdot 10^{-3}$, $5.8 \cdot 10^{-3}$, $6.1 \cdot 10^{-3}$, $6.4 \cdot 10^{-3}$ and $1 \cdot 10^{-2}$ mg mL^{-1}.

Although water is not an ideal solvent for this study, it was chosen to obtain stable dispersions of RBF during the whole complexation process. The increase in the concentration of nanotubes results in an enhancement in the absorbance spectrum of RBF due to the superposition of the two absorbance spectra (Figure 4). On the other hand, blueshifts in the bands at 374 and 444 nm are observed on increasing the nanotube concentration (Figure 4). The shifts are 16 nm for the first band and 11 nm for the latter. The band at 374 nm is attributed to the *p*-*p** and n-*p** transition of RBF and the band at 444 nm to the *p*-*p** transition.[46] The peak at 444 nm hardly changes when the hydrogen-bonding interactions between RBF and its environment change, whereas the maximum at 374 nm does exhibit shifts in the wavelength.[47] The small movements in our system are consistent with reported data[39,48] and confirm the existence of supramolecular interactions in our complex. In addition, the more marked shift of the peak at 374 nm corroborates the modification of the hydrogen-bonding environment of the RBF.

Fluorescence spectroscopy is a more sensitive technique than UV/Vis spectroscopy. Hence, the interaction between the triazine-functionalised carbon nanotubes MWCNTs-3 and RBF was also analysed by using this technique. The effect of increasing the concentrations of MWCNTs-3 on the emission properties of RBF is shown in Figure 5. As one would expect, the addition of MWCNTs-3 to the solution of RBF resulted in

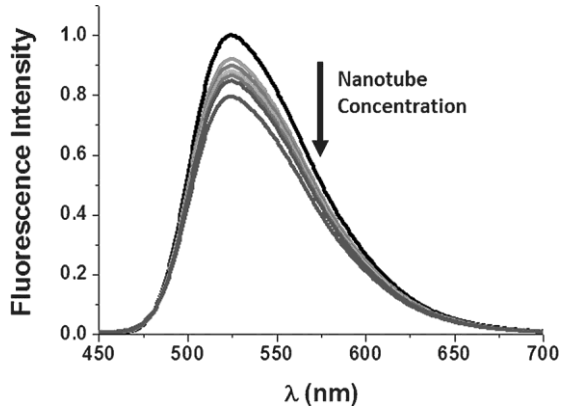

Figure 5. Fluorescence spectra showing a monotonic decrease in intensity of RBF on increasing the concentration of MWCNTs-3 (l_{exc} = 444 nm). [RBF] = $1.0\cdot10^{-3}$ mg mL^{-1}, [MWCNTs-3] = $5.7\cdot10^{-4}$, $7.5\cdot10^{-4}$, $8.9\cdot10^{-4}$, $1\cdot10^{-3}$, $1.3\cdot10^{-3}$ and $2\cdot10^{-3}$ mgmL^{-1}.

partial quenching of its fluorescence emission because of the interaction between the two species.

The maximum of the emission spectrum at 524 nm was used to analyse the quenching data by using the Stern–Volmer equation (1) (Figure S3).[45]

$$F_I^0/F_I = 1+K_{SV}[Q] \quad (1)$$

where F_I^0 and F_I are the fluorescence intensities in the absence and presence of the quencher, respectively, K_{SV} is the Stern–Volmer quenching constant, and [Q] is the concentration of the quencher, MWCNTs-3, in the sample. The Stern–Volmer quenching constant (K_{SV}) was 128.2 6.8 L g^{-1} and this equates to (121.4 6.4)$\cdot10^3$ L mol$_{triazine}^{-1}$. These studies were also carried out with MWCNTs-1, which has fewer triazine chains attached to the walls of the nanotubes. The analysis showed the same trend as observed for the derivative MWCNTs-3. However, MWCNTs-1 exhibited a weaker interaction than MWCNTs-3 because the blueshift in the UV/Vis spectrum was smaller (5 nm at 374 nm and 2 nm at 444 nm) and the quenching of RBF was not very high (Figure S4 and S5). This weaker interaction was confirmed by the association constant calculated from the Stern–Volmer plot (Figure S6). The value was 94.7 4.7 L g^{-1} for the derivative MWCNTs-1.

In molecular systems the association constants between flavins and 2,4-diamino-1,3,5-triazines bound by hydrogen bonds have values between 1 and 744 L mol^{-1},[8,49,50] depending on the substituent(s) on the triazine rings. In addition, the presence of supplementary supramolecular interactions in the system can affect the stabilisation of the hydrogen-bonding interactions and these influences are used to modulate such bonding.[51] As a consequence, the aromatic stacking interactions have been widely studied.[52] Higher association constants between flavins and 2,4-diamino-1,3,5-triazines with different aromatic substituents are observed as a consequence of the increase in the *p*-overlap between these compounds (values from 394 to 17 600 L mol^{-1}).[53] Nanotubes are easily able to form *p*-*p* interactions[54–56] even with flavins[57–62] and the high values of the association constants in our system could be due to the presence of *p*-*p* stacking together with the formation of hydrogen bonds.

A series of nanotube hybrids was studied to analyse the influence that the different kinds of interactions had on the quenching of the fluorescence of RBF. These systems were triazine-functionalised carbon nanotubes with different degrees of functionalisation, i.e., MWCNTs-1 and MWCNTs-3, *p*-tolyl-functionalised carbon nanotubes MWCNTs-2, which cannot form hydrogen bonds, and p-MWCNTs (Figure 6). Pristine nanotubes produced the highest quenching of RBF (black solid line) and the *p*-tolyl-functionalised nanotubes the lowest (line with circles). Presumably, the presence of functional groups in the *p*-tolyl-functionalised carbon nanotubes precludes the approach of the planar rings of RBF to the walls. This situation is consistent with other studies in which a lower quenching effect of functionalised nanotubes was observed when compared with pristine nanotubes.[63] On the other hand, the quenching was higher for the triazine-functionalised carbon nanotubes (solid grey line and line with triangles) in comparison to the *p*-tolyl system (line with circles). Notably, comparison of MWCNTs-3 and MWCNTs-2 shows a far higher quenching for the triazine derivative in comparison to the *p*-tolyl derivative. The fact that both derivatives have similar degrees of functionalisation indicates that the highest quenching can be related to the ability to form hydrogen bonds in the triazine hybrids. The titration of riboflavin with increasing concentrations of MWCNTs-2 gave results that are consistent with this assumption (Figure S7 and S8). The association constant between these two components (riboflavin–MWCNTs-2) is 82.6 5.2 L g^{-1} and this equates to (70.1 4.4)$\cdot10^3$ L mol$_{p\text{-tolyl}}^{-1}$. This value is high because of the possibility of forming *p*-*p* stacking interactions with the functionalised nanotubes but it is lower than that found for the riboflavin–MWCNTs-3 systems; that is, (128.2 6.8) L g^{-1} or (121.4 6.4) 10^3 L mol$_{triazine}^{-1}$. These differences reveal that the hydrogen bonds make a clear contribution to the quenching effect. Similar behaviour has previously been observed in other examples in which the quenching of the fluorescence of flavins is dependent on the ability of their receptors to form hydrogen bonds and *p*-*p* interactions.[64,65] In this way, we demonstrate here that the recognition of the RBF in our system is modulated by the introduction of triazines with the ability to form hydrogen bonds.

Once the formation of complexes between functionalised MWCNTs and RBF had been demonstrated, we carried out some preliminary studies aimed at characterising their electrochemical behaviour in solution. Electrochemical studies on flavins in aqueous solutions are complex and studies concerning interactions with other components are scarce. However, we chose this solvent because of the aforementioned stability of the RBF.

The DPV profiles of $1.0\cdot10^{-3}$ mg mL^{-1} RBF and ($1.0\cdot10^{-3}$–$2.0\cdot10^{-3}$ mg mL^{-1}) RBF-MWCNT hybrids at a bare GCE in 0.1 m phosphate buffer solution pH 7.4 with a scan rate of 0.100 Vs^{-1} are shown in Figure 7. RBF complexes formed with p-MWCNTs and MWCNTs-3 were tested.

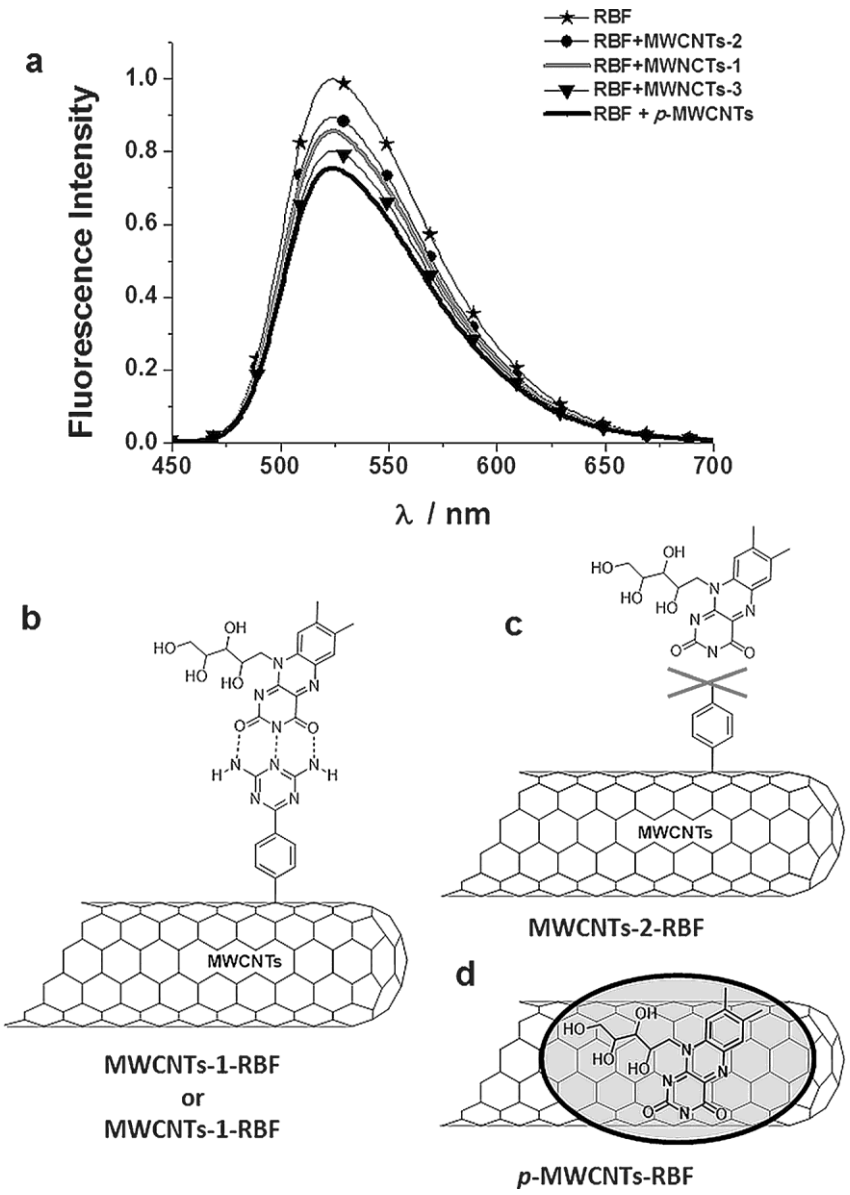

Figure 6. a) Fluorescence spectra of RBF ($1.0 \cdot 10^{-3}$ mgmL^{-1}) and RBF-nanotube ($1.0 \cdot 10^{-3}$–$2.0 \cdot 10^{-3}$ mg mL^{-1}) solutions ($l_{exc} = 444$ nm). Schematic representation of possible structural interactions of RBF with the different hybrids: b) MWCNTs-1 or MWNCTs-3; (c) MWCNTs-2 and (d) p-MWCNTs.

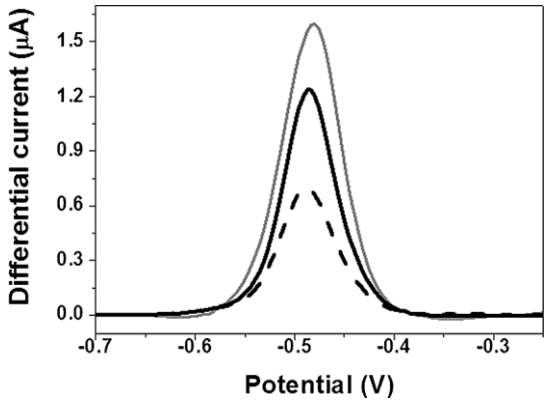

Figure 7. Differential pulse voltammetry of a glassy carbon electrode in RBF (grey solid line), RBF–p-MWCNTs (black solid line), and RBF–MWCNTs-3 (dash line).

Several differences in the intensity and the position of the maximum peak potentials were observed for the compounds. RBF in solution exhibits only one oxidation peak at —0.468 0.006 V and this is in good agreement with the behaviour reported previously.[67] After the interaction of the RBF with p-MWCNTs a shift in the peak potential was not observed (—0.468 0.002 V). Although the quenching of the fluorescence of flavins by aromatic systems has been verified in different studies in which interactions have been demonstrated, *p-p* stacking has not been considered alone as a modulator of the redox behaviour of flavins in solution. Nonetheless, the influence of these interactions on the redox properties of flavins has been widely studied when they participate in complexes involving other noncovalent interactions. However, the effect was not linearly correlated with the *p*-overlap because it is not based on this kind of interaction alone.[52] When RBF interacts

with the derivative MWCNTs-3, a shift of 19 mV in the peak position to more negative potential was observed (—0.487 0.009 V), which indicates that the RBF is more difficult to reduce. The difference of 19 mV in the redox potentials of RBF is in agreement with reported data. Movements of 10–60 mV to more negative potentials have been associated with the stabilisation of the flavin through receptors that are able to take part in both bonding and *p*-*p* stacking.[53]

In light of these preliminary electrochemistry results, the derivative MWCNTs-3 is revealed as a potential hybrid for the modulation of the redox behaviour of RBF. This proposal is consistent with the UV/Vis and fluorescence results and corroborates the influence of the attached organic chains in the systems. Nevertheless, groups that interfere to a greater extent (i.e., strongly electron-withdrawing or electron-donating groups) should be attached to the triazine rings to produce more pronounced variations in the RBF behaviour. In addition, the interaction through hydrogen bonds could become more selective by introducing surfactants that subdue some *p*-*p* interactions.[66]

Conclusion

We have successfully synthesised and characterised 1,3,5-triazine-CNT and *p*-tolyl-CNT derivatives (both SWCNTs and MWCNTs) by means of an aryl radical addition. The self-assembly of these hybrids has been analysed by transmission electron microscopy. It was observed that the 1,3,5-triazine derivatives form good dispersions in water and self-assemble in nonpolar solvents because of the DA-AD hydrogen-bonding recognition, whereas the *p*-tolyl derivatives show better dispersibility in organic solvents and aggregate in polar solvents. On the other hand, the ability of the different nanotubes to recognise RBF has been studied by fluorescence spectroscopy and the scope of the different noncovalent interactions has been analysed. The functionalisation of nanotubes by using a covalent approach decreases their ability to form *p*-*p* stacking interactions, thus allowing hydrogen-bonding interactions to play an important role in the recognition processes between the components. Preliminary electrochemical results show differences in the response of RBF when it interacts with triazine-modified nanotubes.

The possibility of modifying flavin and triazine substituents in our system pave the way for the design of new flavin-based molecular devices as chemical models for flavoenzymes in which recognition and function could be directly correlated.

Experimental Section

Techniques: Microwave irradiation was carried out with a CEM Discover reactor with an infrared pyrometer, pressure control system, stirring and air-cooling option. UV/Vis/NIR spectra were recorded with a Varian Cary 5000 spectrophotometer. Fluorescence spectra were recorded with excitation at 444 nm, an emission filter from 450 to 700 nm and a slit width of 3 nm. For absorption and fluorescence experiments, quartz cuvettes with a 10 mm path-length were used. Fluorescence titration experiments were carried out in water, at RT, by the addition of known microlitre aliquots of a solution containing MWCNTs and RBF ($2\cdot10^{-3}$ mg mL^{-1} and $1\cdot10^{-3}$ mg mL^{-1}, respectively) to 1 mL of a solution containing RBF ($1\cdot10^{-3}$ mg mL^{-1}). UV/Vis titration experiments were carried out in water, at RT, by addition of known microlitre aliquots of a solution containing MWCNTs and RBF ($1\cdot10^{-2}$ mg mL^{-1} and $5\cdot10^{-3}$ mg mL^{-1}, respectively) to 1 mL of a solution containing RBF ($5\cdot10^{-3}$ mg mL^{-1}). The thermogravimetric analyses were performed with a TGA Q50 (TA Instruments) at 10 8C min^{-1} under a N_2 atmosphere. Raman spectra were recorded with an Invia Renishaw microspectrometer equipped with a He-Ne laser at 633 nm excitation wavelength and a laser power of 0.17 mW. For the TEM analyses, several drops of nanotube solutions ($2.5\cdot10^{-2}$ mgmL^{-1}) in different solvents were placed on a copper grid (3.00 mm, 200 mesh, coated with carbon film). After being air-dried, the sample was investigated with a TEM Philips EM 208, accelerating voltage of 100 kV. The NMR spectra were recorded with a Varian Unity 500 MHz spectrometer with TMS as an internal standard. Photoelectron spectra (XPS) were obtained with a VG Escalab 200R spectrometer equipped with a hemispherical electron analyser with a pass energy of 50 eV and a Mg K*a* ($h\nu = 1254.6$ eV) X-ray source, powered at 120 W. Binding energies were calibrated relative to the C 1s peak at 284.8 eV. High-resolution spectra envelopes were obtained by curve fitting synthetic peak components with the software "XPS peak". Symmetric Gaussian–Lorentzian curves were used to approximate the line shapes of the fitting components. Atomic ratios were computed from experimental intensity ratios and normalised by atomic sensitivity factors. Differential pulse voltammetry (DPV) was performed with an Autolab 302b electrochemical workstation (Autolab, The Netherlands). A conventional three-electrode system was employed with a bare Glassy Carbon Electrode (GCE) as working electrode, a platinum wire as auxiliary electrode, and the reference electrode was a saturated Ag/AgCl (3 m KCl). All measurements were performed from —0.7 to 0.4 V using 4 mV step potential and 40 mV as modulation potential, at RT and under a N_2 atmosphere.

Materials: Solvents were purchased from SDS and Fluka. Chemicals were purchased from Sigma–Aldrich and were used as received. HipCo® SWCNTs were purchased from Carbon Nanotechnologies, Inc., Lot R0513 and used without purification. MWCNTs 7000 series were purchased from Nanocyl (lot 31825, www.nanocyl.com) and were used without purification.

Preparation of 6-Amino-2,4-diamine-1,3,5-triazine (1): The preparation of this compound was carried out by using a modified reduction protocol.[68] 6-Nitro-2,4-diamine-1,3,5-triazine (1 g, 4.3 mmol) and hydrazine monohydrate (0.84 mL, 17.2 mmol) were dissolved in EtOH (300 mL) and stirred after the addition of cat. Pd/C (10 %) at 80 8C overnight. The reaction solution was filtered through Celite®, which was washed with ethanol, and the solvent was evaporated under vacuum to give compound 1. Yield: 825 mg (95 %); yellow powder; m.p. 200–202 8C; ^{1}H NMR (500 MHz, [D_6] DMSO, 25 8C): $\delta = 7.96$ (d, J(H,H) = 8.8 Hz, 2H; CH), 6.55 (d, J(H,H) = 8.8 Hz, 2H; CH), 6.48 (s, 4H; NH_2), 5.59 ppm (s, 2 H, NH_2) (Figure S9); ^{13}CNMR (500 MHz, [D_6] DMSO, 25 8C): $\delta = 170.25$ (s, C2), 167.22 (C6), 151.71 (C4'), 129.28 (C2'), 123.93 (C1'), 112.67 ppm (C3') (Figure S10); IR (neat): $\tilde{\nu} = 3700$, 1740, 1734, 1717, 810 cm^{-1} (Figure S11).

Preparation of SWCNTs-1 and MWCNTs-1: Pristine CNTs (25 mg) were sonicated in deionised water together with triazine 1 (210 mg, 1.1 mmol) for 10 min in a microwave glass vessel. Isoamyl nitrite (3) (0.56 mL, 4.16 mmol) was added and a reflux condenser was fitted. The mixture was heated at 80 8C by irradiation at 100 W for 30 min and, after adding a new aliquot of isoamyl nitrite (3), at 30 W for 60 min.[32] The mixture was cooled to RT and

the crude product was filtered off on a Millipore membrane (PTFE, 0.2 *m*m). The product was removed from the filter and washed with dimethylformamide, methanol and dichloromethane (sonicated and filtered) until the filtrate was clear. The solid was finally washed with diethyl ether to afford SWCNTs-1 (23 mg) and MWCNTs-1 (24 mg).

Preparation of SWCNTs-2 and MWCNTs-2: Pristine CNTs (25 mg) were sonicated in deionised water together with *p*-toluidine (2) (120 mg, 1.1 mmol) for 10 min in a microwave glass vessel. Isoamyl nitrite (3) (0.45 mL, 3.34 mmol) was added and a condenser was fitted. The mixture was heated at 80°C by irradiation at 100 W for 30 min and, after adding a new aliquot of isoamyl nitrite (3), at 30 W for 60 min.[32] The mixture was cooled to RT and the crude product was filtered off on a Millipore membrane (PTFE, 0.2 *m*m). The product was removed from the filter and washed with dimethylformamide, methanol and dichloromethane (sonicated and filtered) until the filtrate was clear. The solid was finally washed with diethyl ether to afford SWCNTs-2 (22 mg) and MWCNTs-2 (24 mg).

Acknowledgements

M.V.B. undertook this work with the support of the "ICTP TRIL Programme, Trieste, Italy". Financial support from the Spanish MINECO (projects CTQ2011-22410 and CTQ2014-53600-R), the FEDER Project PEII-2014-002A, the University of Castilla-la Mancha, the University of Trieste and the Italian Ministry of Education MIUR (cofin Prot. 2010N3T9M4 and Firb RBAP11ET-KA) is gratefully acknowledged. We also thank Dr. Emilio M. Pérez for help with Raman spectroscopy.

Keywords: donor–acceptor systems · molecular recognition · nanotubes · noncovalent interactions · receptors

[1] R. Hille, S. Miller, B. Palfey, *Handbook of Flavoproteins*, Berlin/Boston, 2012.
[2] R. F. Carvalhal, R. K. Mendes, L. T. Kubota, *Int. J. Electrochem. Sci.* 2007, *2*, 973–985.
[3] V. Massey, *Biochem. Soc. Trans.* 2000, *28*, 283–296.
[4] M. Mewies, W. S. McIntire, N. S. Scrutton, *Protein Sci.* 1998, /, 7–20.
[5] J. B. Carroll, G. Cooke, J. F. Garety, B. J. Jordan, S. Mabruk, V. M. Rotello, *Chem. Commun.* 2005, 3838–3840.
[6] N. Zainalabdeen, B. Fitzpatrick, M. M. Kareem, V. Nandwana, G. Cooke, V. M. Rotello, *Int. J. Mol. Sci.* 2013, *14*, 7468–7479.
[7] R. Singh, Geetanjali, C. R. Babu, *Chem. Biodiversity* 2005, *2*, 429–446.
[8] R. Deans, G. Cooke, V. M. Rotello, *J. Org. Chem.* 1997, *62*, 836–839.
[9] T. J. Mooibroek, P. Gamez, *Inorg. Chim. Acta* 2007, *360*, 381–404.
[10] B. R. Manzano, F. A. Jalßn, M. L. Soriano, M. C. Carrißn, M. P. Carranza, K. Mereiter, A. M. Rodríguez, A. de La Hoz, A. Sánchez-Migallßn, *Inorg. Chem.* 2008, *4/*, 8957–8971.
[11] P. de Hoog, P. Gamez, I. Mutikainen, U. Turpeinen, J. Reedijk, *Angew. Chem. Int. Ed.* 2004, *43*, 5815–5817; *Angew. Chem.* 2004, *116*, 5939–5941.
[12] B. R. Manzano, F. a. Jalßn, M. L. Soriano, A. M. Rodríguez, A. de La Hoz, A. Sánchez-Migallßn, *Cryst. Growth Des.* 2008, *8*, 1585–1594.
[13] V. Leßn, M. Quintana, M. A. Herrero, J. L. G. Fierro, A. de La Hoz, M. Prato, E. Vázquez, *Chem. Commun.* 2011, *4/*, 10936–10938.
[14] V. Leßn, A. M. Rodriguez, P. Prieto, M. Prato, E. Vázquez, *ACS Nano* 2014, *8*, 563–571.
[15] Á. Díaz-Ortiz, J. Elguero, C. Foces-Foces, A. de La Hoz, A. Moreno, M. del C. Mateo, A. Sánchez-Migallßn, G. Valiente, *New J. Chem.* 2004, *28*, 952–958.
[16] A. Ruiz-Carretero, O. Noguez, T. Herrera, J. R. Ramírez, A. Sánchez-Migallßn, A. de La Hoz, *J. Org. Chem.* 2014, */9*, 4909–4919.
[17] A. Ruiz-Carretero, J. R. Ramírez, A. Sánchez-Migallßn, A. de La Hoz, *Tetrahedron* 2014, */0*, 1733–1739.
[18] Á. Díaz-Ortiz, J. Elguero, A. de La Hoz, A. Jiménez, A. Moreno, S. Moreno, A. Sánchez-Migallßn, *QSAR Comb. Sci.* 2005, *24*, 649–659.
[19] M. D. Greaves, T. H. Galow, V. M. Rotello, *Chem. Commun.* 1999, 169–170.
[20] L. Vial, P. Dumy, *New J. Chem.* 2009, *33*, 939–946.
[21] M. M. Shulaker, G. Hills, N. Patil, H. Wei, H.-Y. Chen, H.-S. P. Wong, S. Mitra, *Nature* 2013, *501*, 526–530.
[22] A. Battigelli, C. Ménard-Moyon, T. Da Ros, M. Prato, A. Bianco, *Adv. Drug Delivery Rev.* 2013, *65*, 1899–1920.
[23] P. Yáñez-Sedeño, J. M. Pingarrßn, J. Riu, F. X. Rius, *TrAC Trends Anal. Chem.* 2010, *29*, 939–953.
[24] P. M. Ajayan, *Chem. Rev.* 1999, *99*, 1787–1800.
[25] P. Singh, S. Campidelli, S. Giordani, D. Bonifazi, A. Bianco, M. Prato, *Chem. Soc. Rev.* 2009, *38*, 2214–2230.
[26] A. Micoli, M. Quintana, M. Prato, *Supramol. Chem.* 2013, *25*, 567–573.
[27] J. Wang, *Electroanalysis* 2005, *1/*, 7–14.
[28] G. Ke, *Carbohydr. Polym.* 2010, */9*, 775–782.
[29] L. A. S. D. A. Prado, A. De La Vega, J. Sumfleth, K. Schulte, *J. Polym. Sci. Part B* 2009, *4/*, 1860–1868.
[30] S. S. Mahapatra, S. K. Yadav, H. J. Yoo, J. W. Cho, J.-S. Park, *Composites Part B* 2013, *45*, 165–171.
[31] R. K. Saini, I. W. Chiang, H. Peng, R. E. Smalley, W. E. Billups, R. H. Hauge, J. L. Margrave, *J. Am. Chem. Soc.* 2003, *125*, 3617–3621.
[32] F. G. Brunetti, M. A. Herrero, J. D. M. Muñoz, A. Díaz-Ortiz, J. Alfonsi, M. Meneghetti, M. Prato, E. Vázquez, *J. Am. Chem. Soc.* 2008, *130*, 8094–8100.
[33] M. E. Lipin´ska, S. L. H. Rebelo, M. F. R. Pereira, J. a. N. F. Gomes, C. Freire, J. L. Figueiredo, *Carbon* 2012, *50*, 3280–3294.
[34] J. L. Bahr, J. Yang, D. V. Kosynkin, M. J. Bronikowski, R. E. Smalley, J. M. Tour, *J. Am. Chem. Soc.* 2001, *123*, 6536–6542.
[35] R. Graupner, *J. Raman Spectrosc.* 2007, *38*, 673–683.
[36] S. Giordani, J.-F. Colomer, F. Cattaruzza, J. Alfonsi, M. Meneghetti, M. Prato, D. Bonifazi, *Carbon* 2009, *4/*, 578–588.
[37] M. Quintana, M. Prato, *Chem. Commun.* 2009, 6005–6007.
[38] M. D. Greaves, V. M. Rotello, *J. Am. Chem. Soc.* 1997, *119*, 10569–10572.
[39] S. Dutta Choudhury, J. Mohanty, A. C. Bhasikuttan, H. Pal, *J. Phys. Chem. B* 2010, *114*, 10717–10727.
[40] B. J. Jordan, G. Cooke, J. F. Garety, M. A. Pollier, N. Kryvokhyzha, A. Bayir, G. Rabani, V. M. Rotello, *Chem. Commun.* 2007, 1248–1250.
[41] K. Ariga, A. Kamino, H. Koyano, T. Kunitake, *J. Mater. Chem.* 1997, /, 1155–1161.
[42] E. Breinlinger, A. Niemz, V. M. Rotello, *J. Am. Chem. Soc.* 1995, *11/*, 5379–5380.
[43] G. Weber, *Biochem. J.* 1950, *4/*, 114–121.
[44] M. Quick, A. Weigel, N. P. Ernsting, *J. Phys. Chem. B* 2013, *11/*, 5441–5447.
[45] V. V. Mokashi, L. S. Walekar, P. V. Anbhule, S. H. Lee, S. R. Patil, G. B. Kolekar, *J. Nanopart. Res.* 2014, *16*, 2291.
[46] P. F. Heelis, *Chem. Soc. Rev.* 1982, *11*, 15–39.
[47] K. Yagi, N. Ohishi, K. Nishimoto, J. Do Choi, P.-S. Song, *Biochemistry* 1980, *19*, 1553–1557.
[48] A. Saha, S. Manna, A. K. Nandi, *Langmuir* 2007, *23*, 13126–13135.
[49] E. Jeoung, H. Augier de Cremiers, R. Deans, G. Cooke, S. L. Heath, P. E. Vanderstraeten, V. M. Rotello, *Tetrahedron Lett.* 2001, *42*, 7357–7359.
[50] R. Deans, A. O. Cuello, T. H. Galow, M. Ober, V. M. Rotello, *J. Chem. Soc. Perkin Trans. 2* 2000, 1309–1313.
[51] G. Cooke, V. M. Rotello, *Chem. Soc. Rev.* 2002, *31*, 275–286.
[52] V. Nandwana, I. Samuel, G. Cooke, V. M. Rotello, *Acc. Chem. Res.* 2013, *46*, 1000–1009.
[53] E. C. Breinlinger, V. M. Rotello, *J. Am. Chem. Soc.* 1997, *119*, 1165–1166.
[54] A. Mateo-Alonso, C. Ehli, K. H. Chen, D. M. Guldi, M. Prato, *J. Phys. Chem. A* 2007, *111*, 12669–12673.
[55] S.-N. Ding, D. Shan, S. Cosnier, A. Le Goff, *Chem. Eur. J.* 2012, *18*, 11564–11568.
[56] P. D. Petrov, G. L. Georgiev, A. H. E. Müller, *Polymer* 2012, *53*, 5502–5506.
[57] C. S. Lin, R. Q. Zhang, T. A. Niehaus, T. Frauenheim, *J. Phys. Chem. C* 2007, *111*, 4069–4073.

[58] S.-Y. Ju, J. Doll, I. Sharma, F. Papadimitrakopoulos, *Nat. Nanotechnol.* 2008, *3*, 356–362.
[59] S.-Y. Ju, D. C. Abanulo, C. A. Badalucco, J. A. Gascßn, F. Papadimitrakopoulos, *J. Am. Chem. Soc.* 2012, *134*, 13196–13199.
[60] S. Ju, F. Papadimitrakopoulos, *J. Am. Chem. Soc.* 2008, *130*, 655–664.
[61] R. Sharifi, D. C. Abanulo, F. Papadimitrakopoulos, *Langmuir* 2013, *29*, 7209–7215.
[62] J. Sim, H. Oh, E. Koo, S.-Y. Ju, *Phys. Chem. Chem. Phys.* 2013, *15*, 19169–19179.
[63] D. K. Singh, P. K. Iyer, P. K. Giri, *Carbon* 2012, *50*, 4495–4505.
[64] C. Subramani, G. Yesilbag, B. J. Jordan, X. Li, A. Khorasani, G. Cooke, A. Sanyal, V. M. Rotello, *Chem. Commun.* 2010, *46*, 2067–2069.
[65] J. Carroll, M. Gray, K. Bardon, H. Nakade, V. Rotello, *Lett. Org. Chem.* 2004, *1*, 227–230.
[66] A. Di Crescenzo, V. Ettorre, A. Fontana, *Beilstein J. Nanotechnol.* 2014, *5*, 1675–1690.
[67] H. Zhang, J. Zhao, H. Liu, H. Wang, R. Liu, J. Liu, *Int. J. Electrochem. Sci.* 2010, *5*, 295–301.
[68] H. Weissauer, W. Braun, A. Tratter, *Dyestuffs Containing Diamino Triazine Groups*, 1965.